The characteristics of the Drop Size Distribution revealed from TEAM-R polarimetric radar observation in the stratiform and convective rain of typhoon Fanapi(2010)

Pei-Yu Huang, , TaiChi Chen Wang, Yu-Chieng Liou, and Xin-Hao Liao

Institute of Atmospheric Physic, National Central University

1. Background

Near 00 UTC, Sep.19 Typhoon Fanapi (2010) was approaching the east coast of Taiwan and made its landfall(Fig.1). A mobile X-band dual polarization / Doppler radar, TEAM-R (Taiwan Experimental Atmospheric Mobil Radar) had been deployed at southern Taiwan on Sep 18, together with the other three operational radars(Fig.2), providing opportunity to observe the re-organizing process on Sep 19. Fanapi went through a reorganizing process and brought heavy rainfall in southwest Taiwan(Fig.3). For the closer look of the reorganizing process the one hour reflectivity time series of Chigu radar is illustrated in Fig. 4. The goal in this study is getting more information from mobile Doppler/dual-polarimetric radar to study the microphysical characteristics. In addition, to compare the DSDs from the long-lived strong convective rainband and the newly formed eye wall.

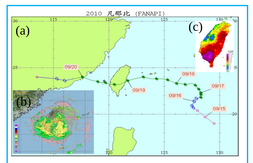

Fig.1 (a) Track determined by Central Weather Bureau, Taiwan. (b) The mosaic reflectivity at 03 UTC. (c) Accumulate rainfall during Typhoon Fanapi.

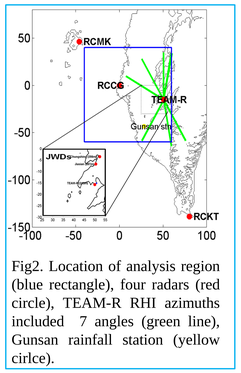

Fig2. Location of analysis region (blue rectangle), four radars (red circle), TEAM-R RHI azimuths included 7 angles (green line), Gunsan rainfall station (yellow cirlce).

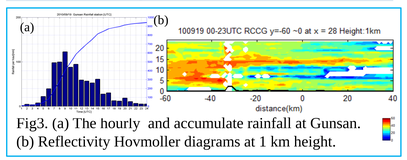

Fig3. (a) The hourly and accumulate rainfall at Gunsan. (b) Reflectivity Hovmoller diagrams at 1 km height.

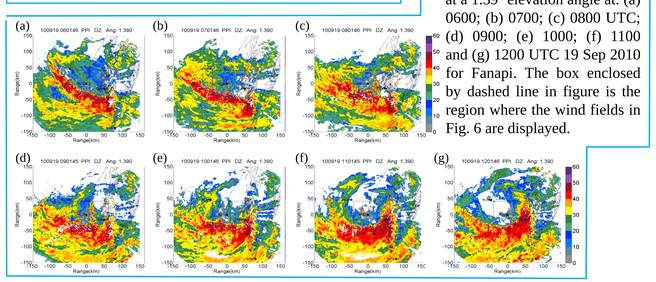

Fig 4 Radar reflectivity (5 dBZ intervals) observed by RCCG at a 1.39º elevation angle at: (a) 0600; (b) 0700; (c) 0800 UTC; (d) 0900; (e) 1000; (f) 1100 and (g) 1200 UTC 19 Sep 2010 for Fanapi. The box enclosed by dashed line in figure is the region where the wind fields in Fig. 6 are displayed.

2. Methods and Tools

We used a variational-based multi-Doppler radars synthesis method proposed by Liou and Chang (2009) and Liou et al. (2012) , named WInd Synthesis System using DOppler Measurements (WISSDOM), it can construct the three dimensional wind field over complex topography. All the radar data had been corrected by Software, name Rakit, that design by our team. The procedure of DSD retried from radar showed below:

get one μ- Λ relation from observation data of JWD → select the axis ratio to get one set of ZDR-μ relations → verification → used this table in retrieved DSD by the dual-polarization radar

3. The dynamic features during re-organizing process

3.1 The kinematic and thermodynamic field evolution

We select three time stages: 0601, 0948 and 1201 to illustrate the changes of the kinematic fields. Fig. 5 showed the horizontal wind, reflectivity , isotach, vertical motion and vertical vorticity at 2 km height.

At 06 UTC , a strong rain band (Fig.5a) was formed by the convergence between the NNW and the outer circulation which was less infected by the terrain. By 0948, a vortex can be clearly identified on the west side of foot hill. Near 1201, the tangetial wind was incresed to 30 m/sec (Fig.5b). The vertical motion can reached 6 m/sec along the newly formed eyewall. (Fig.5c) The time series of the vorticity field indicated the spin up progress during the reorganizing stage. (Fig.5d) The retrieved perturbation pressure (Fig.6) and the temperature field at 0948 also illustrated the warm core low center associated with the reforming eye wall and tangential circulation.

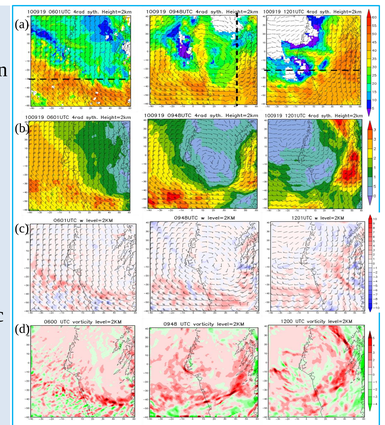

Fig.5 The multiple-Doppler radar synthesized wind fields result at Z=2 km ASL. The shading means (a) reflectivity , (b) isotach, (c) vertical motion and (d) vertical vorticity.

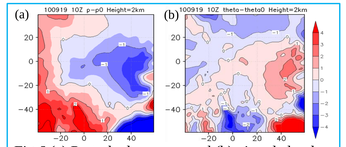

Fig.6 (a) Perturbed pressure and (b) virtual cloud equivalent temperature and at 2km in 09-12UTC.

3.2 The reformed eye wall

Through the period of rain band and re-organizing period eye wall, we observed many deep hot towers. Fig. 7 showed vertical motion and refectivity of three cross sections at the same time periods in 3.1. The strong updrafts (>5m/sec) and downdraft (>2m/sec) associated with the vertical erected reflectivity core (>45dBz). At 0948 and 1201, the flow pattern is very similar to the the conceptual model of Willoughby, 1998.

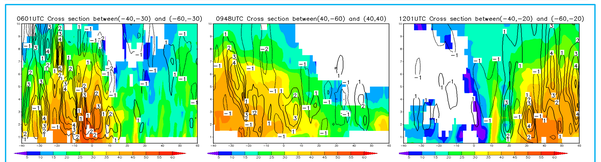

Fig.7 The cross section reflectivity (shading) and vertical motion (contour). (a) 0601UTC at Y=-30. (b) 0948UTC at Y=40. (c) 1201 UTC at Y=-20. (See Fig.6a dash line marked the location of these cross section)

3.3 The initiation of the south wind near the foothill by topographic effect

We noticed the south wind at low level near the foot hill at 0800 UTC and initiate the strong eye wall vortex circulation in the next 4 hours. However how did this south wind start to evolve? From 0500UTC to 0800 UTC the NW wind from the typhoon circulation slowly weaken near the foot hill, finally at lowest level the weak wind to the north side of the rain band was not able to climb over the terrain and turn toward north instead. The Froude no on 08 UTC was 0.35. This phenomena can also be seen on the RHI observation from TEAM –R (Fig.8) showing the weak south wind in this area. We can clearly see the extension of the enhancing south wind from low level to higher level. This also provide a good proof of the bottom-up spin up process of the reformed eye wall.

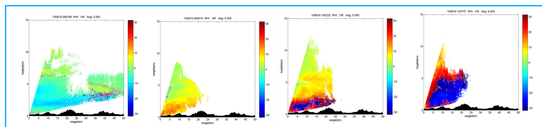

Fig.8 Radial wind field from TEAM-R RHI 0 degree azimuth angle (toward north from 0600 to 1200 UTC. (We show the raw data with folded wind for easier identification of the strong wind)

4. The DSD characteristics of the reorganizing eye wall

A Joss-Waldvogel disdrometer near the TEAM-radar site had collected the DSD data during 19 Sep. 2010. We use this data set and T-matrix software to test our polarimetric radar retrieval DSD algorithm. We apply a similar method of Zhang and Brandes (2002) to retrieve DSD, the result indicated a well match. During heavy rainfall, radar retrieved DSD have slightly higher NW and smaller DM (Fig.9). With confidence from this result, all the polarimetric observations including PPI and RHI were processed to get the DSD distributions.

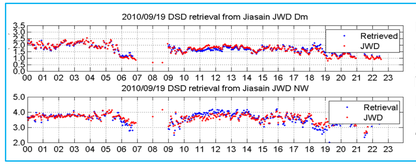

Fig.9 Verified the accuracy of the polarimetric radar drop size retrieval scheme by comparing disdrometers DSD data and T-matrix scattering model at near TEAM-R .

4.1 Rainband Stage

From 06:00 to 07:00 UTC, many hot towers were embedded near the northern edge of a NW-SE strong stationary rain band (Fig.4a). The retrieved DSD PPI distribution from TEAM-R were shown in (Fig 10). We notice very large Dm(~3.5mm) and high Nw(~10^4.5) associated with the strong vertical motion(~5m/s) in this convective region (reflectivity > 30dBz). The RHI results for the eight different times in 7.5 minutes interval have very similar pattern. We can clearly see the high tower with strong vertical motion can provide the chance for the larger rain drop to form with the bounty supply of the smaller droplets horizontal convergence (Fig.10).

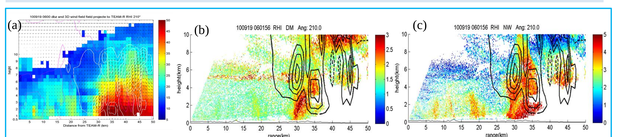

Fig.10 (a) Reflectivity (dBz) . (b) Mass-weighted mean diameter (Dm). (c) Intercept parameter (Nw) observed and retrieved by TEAM-R at a 1.50o elevation angle at 0604 UTC.

4.2 Newly formed eye wall stage

From 12:00 to 13:00 UTC, the newly reorganizing eyewall was developing in this region(Fig.4g), the strong attenuation limited the retrieval coverage(Fig. 11). However, the Retrieved DSD still provide very different characteristics , an even higher NW were observed through the hour , the Dm were generally smaller than the Dm from rainband stage data. The very high Nw indicated there are many newly formed droplets and tiny raindrops provided the large amount of latent heat to intensify the eye wall circulation.

The same characteristics can be easily seen from scatter plot (Fig. 12): Higher Nw and smaller Dm for the newly formed eye wall stage; Larger Dm for the stationary rain band stage. If we plot all these DSD results to compare with the Bringi et al. (2003) DSD for marine and continental convections, as we found in other typhoon cases (Chang et al., 2009) , we found the DSDs are located between the marine and continental types. However, the DSD of rain band stage is closer to continental type, while the DSDs of the newly formed eyewall is closer to the marine type instead. And we also found such different between stratiform precipitation and convection precipitation in Dm-Nw scatter-plot(Fig.13) in this study.

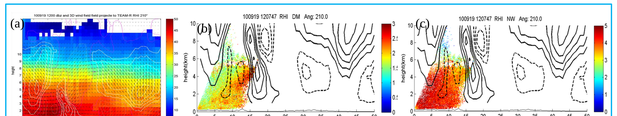

Fig.11 Same as Fig.14, but at 1201 UTC

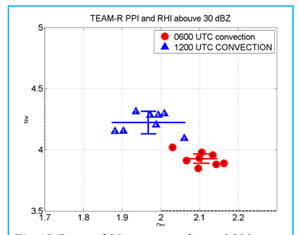

Fig.12 Dm and Nw scatter plot at 0600-0700 UTC (red point) and 1200-1300 UTC (blue triangle). Each point was calculated by one PPI data and one RHI data at nearest time, the time interval is about 10 minutes.

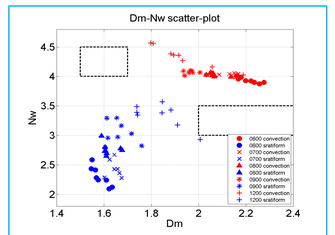

Fig.13 Dm and Nw scatter plot from 0600 to 1200 UTC. Blue notation mark stratiform classification that below 35 dBZ, and red mark the convection that above 35dBZ. Each point was calculated by one 0.5 degree PPI data.

5. Conclusion

1. The radar network at southern Taiwan and a mobile polarimetric radar (TEAM-R) had closely observed its structure change during the re-organizing stage of Typhoon Fanapi .
2. The kinematic and thermodynamic fields were retrieved from multiple Doppler synthesis. The consistent results indicated a warm core low pressure center associated with the newly formed eye. The eye wall characteristics is also observed from the vertical cross section.
3. The Doppler wind field showed the tangential wind was initiated near the lowest level, its intensity was increasing and extending to upper levels in a few hours. The central mountain ridge may play an important role of the initiation of the tangential wind component by blocking.
4. The retrieved DSDs from X-band polarimetric radar has shown very different characteristics between the rain band stage and newly formed eye wall. The enormous Nw for the high concentration of smaller rain drops at the eye wall developing stage provide a clue for intensification from latent heat release.

Reference

Bringi, V.N., V. Chandrasekar, J. Hubert, E. Gorgucci, W. Randeu, and M. Scoenhuber, 2003a: Raindrop size distribution in different climate regimes from disdrometer and dual-polarized radar analysis. J. Atmos. Sci., 60, 354-365.
Chang, W. Y., T.-C. Chen Wang, and P.-L. Lin,2009: Characteristics of the Raindrop Size Distribution and Drop Shape Relation in Typhoon Systems in the Western Pacific from the 2D Video Disdrometer and NCU C-Band Polarimetric Radar. J. Atmos. Oceanic Technol., 26, 1973-1993
Liou, Y.-C., S.-F. Chang, and J. Sun, 2012: An application of the immersed boundary method for recovering the three-dimensional wind fields over complex terrain using multiple-Doppler radar data. Mon. Wea. Rev., 40, 1603-1619.
Shapiro, L.J., and H.E. Willoughby, 1982: The response of balanced hurricanes to local sources of heat and momentum. J. Atmos. Sci., 39, 378-394.
Willoughby, H.E., 1998: Tropical Cyclone Eye Thermodynamics. Mon. Wea. Rev., 126, 3053-3067
Zhang, G., J. Vivekanandan, and E. Brandes, 2001: A method for estimating rain rate and drop size distribution from polarimetric radar measurements. IEEE Trans. Geosci. Remote Sens., 39, 830-841

Acknowledgment

This research is supported by the Ministry of Science and Technology of Taiwan, under MOST104-2119-M-492-005 and MOST103-2625-M-008-007-MY2. Special thanks go to the crew members who operated the S-POL, RCCG, RCKT, RCWF and TEAM-R.